

# From Networks of Unstable Attractors to Heteroclinic Switching

Christoph Kirst<sup>1-4</sup> and Marc Timme<sup>1,2</sup>

<sup>1</sup>*Network Dynamics Group, Max Planck Institute for Dynamics and Self-Organization (MPIDS) and*

<sup>2</sup>*Bernstein Center for Computational Neuroscience (BCCN) Göttingen, 37073 Göttingen, Germany*

<sup>3</sup>*Fakultät für Physik, Georg-August-Universität Göttingen, Germany*

<sup>4</sup>*DAMTP, Centre for Mathematical Sciences, Cambridge University, Cambridge CB3 0WA, UK*

We present a dynamical system that naturally exhibits two unstable attractors that are completely enclosed by each others basin volume. This counter-intuitive phenomenon occurs in networks of pulse-coupled oscillators with delayed interactions. We analytically show that upon continuously removing a local non-invertibility of the system, the two unstable attractors become a set of two non-attracting saddle states that are heteroclinically connected. This transition equally occurs from larger networks of unstable attractors to heteroclinic structures and constitutes a new type of singular bifurcation in dynamical systems.

PACS numbers: 05.45.Xt, 02.30.Oz,

The concepts of attractor and stability are at the core of dynamical systems theory [1] because attractivity and stability determine the long term behavior and often the typical properties of a system. Attraction and stability which may change via bifurcations are thus fundamental to modeling in all of science and engineering. For systems with smooth and invertible flows these concepts have long been studied and are well understood, allowing classifications of dynamical systems and their bifurcations, for example by using topological equivalence and normal forms.

Dynamical systems with non-smooth or non-invertible flows, such as hybrid or Fillipov systems [2], are far less understood although they model a variety of natural phenomena, ranging from the mechanics of stick-slip motion and the switching dynamics of electrical circuits, to the generation of earthquakes and the spiking activity of neural networks [3, 4, 5]. For instance, spiking neurons interact by sending and receiving electrical pulses at discrete instances of time that interrupt the intermediate smooth interaction-free dynamics. This neural dynamics and similarly that of, e.g., cardiac pacemaker cells, plate tectonics in earthquakes, chirping crickets and flashing fireflies are often modeled as pulse-coupled oscillators.

Such hybrid systems display dynamics very different from that of temporally continuous or temporally discrete systems. Networks of oscillators with global homogeneous delayed pulse-coupling may robustly exhibit *unstable attractors* [5] (invariant periodic orbits that are Milnor attractors [1] but locally unstable). In the presence of noise, these systems exhibit a dynamics akin to heteroclinic switching [6], a feature that is functionally relevant in many natural systems such as in neural, weather and population dynamics [6, 7]. Rigorous analysis [8] shows that invertible systems in general cannot have unstable attractors and that a saddle state can in principle be converted to an unstable attractor by locally adding a non-invertible dynamics onto the stable manifold. However, the potential relation of unstable at-

tractors to heteroclinic cycles is not well understood and it is unknown whether and how unstable attractors may be created or destroyed via bifurcations.

In a network of pulse-coupled oscillators we here demonstrate the existence of two unstable attractors that are enclosed by the basin of attraction of each other. We explain this counter-intuitive phenomenon: Continuously lifting the local non-invertibility of the system with two unstable attractors creates a standard heteroclinic two-cycle. This transition equally occurs from large networks of unstable attractors to heteroclinic structures and constitutes a new type of singular bifurcation in hybrid dynamical systems.

We consider a network of  $N$  oscillatory units with a state defined by a phase-like variable  $\phi_i(t) \in \mathbb{R}$ ,  $i \in \{1, 2, \dots, N\}$ , that increases uniformly in time  $t$

$$\frac{d}{dt}\phi_i = 1. \quad (1)$$

Upon crossing a threshold at time  $t_s$ ,  $\phi_i(t_s) \geq 1$ , unit  $i$  is instantaneously reset,

$$\phi_i(t_s^+) := \lim_{r \searrow 0} \phi_i(t_s + r) = K(\phi_i(t_s)). \quad (2)$$

Here  $K(\phi) = U^{-1}(R(U(\phi) - 1))$  is determined by a smooth, unbounded, strictly monotonic increasing *rise function*  $U(\phi)$  normalized to  $U(0) = 0$  and  $U(1) = 1$  and a smooth non-negative *reset function*  $R$  satisfying  $R(0) = 0$ . In addition to the reset (2) a pulse is sent which is received by all units  $j$  after a delay time  $\tau > 0$ , inducing a phase jump

$$\phi_j(t_s + \tau) = H_{\varepsilon_{ji}}\left(\phi_j\left((t_s + \tau)^-\right)\right) \quad (3)$$

with *interaction function*  $H_\varepsilon(\phi) = U^{-1}(U(\phi) + \varepsilon)$  and coupling strength  $\varepsilon_{ji}$  from unit  $i$  to unit  $j$ . We set  $J_\varepsilon(\phi) = K \circ H_\varepsilon(\phi)$  and denote a phase shift by  $S_\eta(\phi) = \phi + \eta$ .

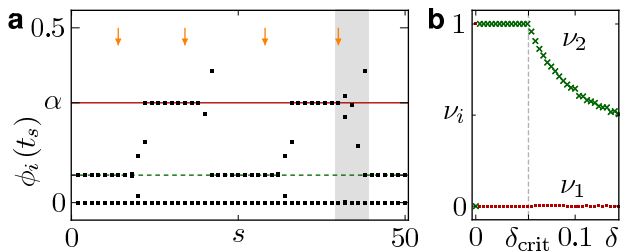


Figure 1: (color online) Two unstable attractors enclosed by the basins of each other ( $c = 0$ ). **(a)** Phases  $\phi_i(t_s)$  (dots) of all units at times  $t_s$  just after the  $s$ -th reset of a reference unit  $i = 1$ . Lines indicate the phases on the invariant orbit  $A_1$  ( $\alpha$ , solid) and  $A_2$  (dashed). Arrows mark times of small phase perturbations which induce switches from  $A_1$  to  $A_2$  or vice versa. The shaded area highlights a switch from  $A_1$  to  $A_2$  that is shown in detail in Fig. 2. **(b)** Fraction  $\nu_i$  of 5000 trajectories reaching the periodic orbit  $A_i$  ( $\bullet$  :  $i = 1$ ,  $\times$  :  $i = 2$ ) starting from random phases distributed uniformly in a box of side width  $2\delta$  centered around  $\phi = a_1$  on the orbit  $A_1$ . For  $0 < \delta < \delta_{\text{crit}} \approx 0.05$  all trajectories reach the orbit  $A_2$  ( $\nu_2 = 1$ ), indicating that  $A_1$  is enclosed by the basin volume of  $A_2$  and in particular that  $A_1$  is an unstable attractor.

This system represents, for instance, an abstract model of neuronal oscillators with a membrane potential  $u_i(t) = U(\phi_i(t))$ . The neurons' responses to inputs are described by increasing the potentials instantaneously by an amount  $\varepsilon_{ij}$ , that represents the transferred charge from the pulse sending (presynaptic) neuron  $j$  to the pulse receiving (postsynaptic) one  $i$ . If this input is supra-threshold,  $u_i(t) = u_i(t^-) + \varepsilon_{ij} > 1$ , unit  $i$  is *partially reset* to

$$u_i(t^+) = R(u_i(t) - 1) \geq 0. \quad (4)$$

This accounts for remaining synaptic input charges which are not used to reach the threshold and which contribute to the potential after reset [9]. For  $R(\zeta) \equiv 0$  we recover the model analyzed in previous studies [5] which has a local non-invertibility since the original phase of a unit cannot be recovered after it received supra-threshold input and was reset to  $J_\varepsilon(\phi) \equiv 0$ . For an invertible  $R$  the flow becomes locally time invertible.

Here we focus on a homogeneous network of all-to-all coupled excitatory units without self-interaction, i.e.  $\varepsilon_{ij} = (1 - \delta_{ij})\varepsilon$ ,  $\varepsilon > 0$ . The permutation symmetry implies invariant subspaces of two or more synchronized units and thus the possibility of robust heteroclinic cycles, cf. [10]. For the numerical simulations presented below we fix  $\varepsilon = 0.23$ ,  $\tau = 0.02$ , a rise function  $U(\phi) = \frac{1}{b} \log(1 + (\exp(b) - 1)\phi)$  with  $b = 4.2$  and partial reset  $R(\zeta) = c\zeta$  with parameter  $c \in [0, 1]$  which is invertible for all  $c > 0$ . For these parameters the model exhibits short switching times between periodic orbits which simplifies the presentation of the analysis below; however, the studied phenomena is robust against structural perturbations in  $\tau$ ,  $\varepsilon$  and the function  $U$ .

For locally non-invertible dynamics ( $c = 0$ ) the above system exhibits unstable attractors in a large fraction of parameter space and for different network sizes  $N$  [5, 8]. For the above parameters, the smallest system in which we observed unstable attractors has  $N = 4$  units. Curiously, numerical simulations, e.g. Fig. 1a, indicate that such a system exhibits two unstable attractors each of which is fully enclosed by the basin volume of the other attractor, Fig. 1b.

We confirm these numerical findings analytically. Given a periodic orbit  $A$ , define the basin of attraction  $\mathcal{B}(A)$  as the set of points in state space that converge to  $A$  in the long time limit. Below we show that in the system (1)-(3) with  $R(\zeta) \equiv 0$  there is a pair of periodic orbits  $A_1$  and  $A_2$  such that a full measure set of points of an open neighborhood of  $A_1$  is contained in the basin  $\mathcal{B}(A_2)$  and vice versa.

To study the dynamics in detail we use an event based analysis, cf. e.g. [4]. The event when a unit  $i$  sends a pulse is denoted by  $s_i$ , the reception of a pulse from unit  $j$  by  $r_j$  and simultaneous events are enclosed in parentheses. For given parameter  $c \in [0, 1]$ , a simple saddle periodic orbit  $A_1$  (cf. Figs. 1a and 3a) is uniquely determined by the cyclic event sequence

$$E(A_1) = (s_1, s_2)(r_1, r_2, s_3, s_4)(r_3, r_4) \quad (5)$$

By exchanging the indices  $(1, 2) \leftrightarrow (3, 4)$  in (5) we obtain the event sequence of a permutation equivalent periodic orbit  $A_2$ . Both orbits lie in the intersection of the two invariant subspaces  $\{\phi_1 = \phi_2\}$  and  $\{\phi_3 = \phi_4\}$  with synchronized units  $(1, 2)$  and  $(3, 4)$ , respectively, allowing a robust heteroclinic connection between them. As it turns out below the local stability and non-local attractivity properties of the  $A_i$  depend on the parameter  $c$ .

We now first locally reduce the infinite dimensional state space of the hybrid dynamical system with delayed coupling to three dimensions: Local to  $A_1$  and  $A_2$  the state space reduces in finite time [8] to an eight-dimensional state space spanned by the four phases  $\phi = (\phi_1, \phi_2, \phi_3, \phi_4)$ , and the four times  $\sigma_i \geq 0$ ,  $i \in \{1, \dots, 4\}$  elapsed since the most recent pulse generation of oscillator  $i$ . We consider the subset  $\mathcal{M} = \{(\phi, \sigma) \mid \sigma_i > \tau, i \in \{1, \dots, 4\}\}$  of the state space where all pulses have been received: Then the state space is effectively four dimensional, since the exact values of the  $\sigma_i > \tau$  do not influence the dynamics. Due to the uniform phase shift (1),  $A_1$  is a straight line in  $\mathcal{M}$  after the last and before the first event in the sequence (5). We denote the point in the center of this line by  $a_1$  and consider states with phases  $\phi = a_1 + (\delta_1, \delta_2, \delta_3, \delta_4)$  in a neighborhood. Because of shift invariance we may further fix  $\delta_1 = 0$ , being left with a locally three-dimensional representation  $\mathcal{P}_1 \subset \mathbb{R}^3$  of the original state space with states  $(\delta_2, \delta_3, \delta_4) \in \mathcal{P}_1$ . Similarly, we have a local three-dimensional representation  $(\delta_4, \delta_1, \delta_2) \in \mathcal{P}_2$  of the state space around  $a_2 \in \mathcal{M} \cap A_2$ , constructed analogously to

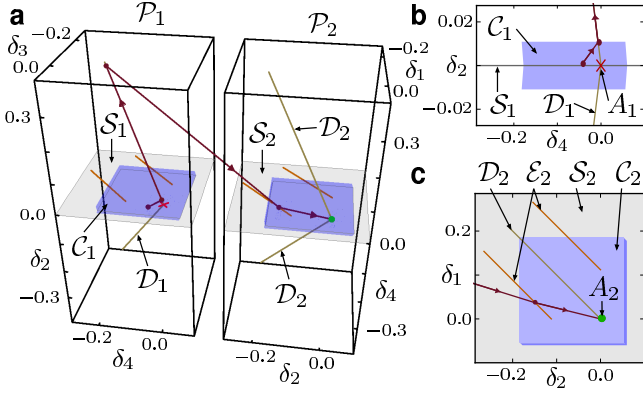


Figure 2: (color online) Structure of the three-dimensional reduced state space for  $c = 0$  showing that the  $A_i$  are unstable attractors enclosed by the basins of each other. (a) Representations  $\mathcal{P}_i$  of the state space in a neighborhood of  $A_1 \in \mathcal{P}_1$  (cross) and  $A_2 \in \mathcal{P}_2$  (ball). All trajectories starting in the set  $\mathcal{C}_1$  (close to  $A_1$ ) lead to a switch to  $A_2$ . The line with arrows shows a sample trajectory of the marked switch from  $A_1$  to  $A_2$  in Fig. 1a. (b) Projection of  $\mathcal{P}_1$  onto the  $\delta_2$ - $\delta_4$  plane and (c) of  $\mathcal{P}_2$  onto the  $\delta_1$ - $\delta_2$  plane, illustrating that, except for the lower dimensional subset  $\mathcal{S}_i$ , the attractor  $A_i$  is enclosed by  $\mathcal{C}_i$ , i.e. the  $A_i$  are unstable attractors.

$a_1$ , this time fixing  $\delta_3 = 0$ . There is an open neighborhood of  $A_i$  in the full eight-dimensional state space from which every orbit crosses  $\mathcal{P}_i$  after at most eight events (one cycle). In this sense  $\mathcal{P}_i$  is a three-dimensional Poincaré section in a neighborhood of  $A_i$ .

For arbitrary  $c \in [0, 1]$  there are regions in  $\mathcal{P}_1$  and  $\mathcal{P}_2$  from which all trajectories evolve back to points in either  $\mathcal{P}_1$  or  $\mathcal{P}_2$ . Between these regions we derive return maps and their domains which follow directly from the definition of the local state space and the event sequence (Fig. 2 visualizes domains of the key maps and a sample trajectory for  $c = 0$ ). For instance, the orbit  $A_1$  is enclosed by the three-dimensional domain  $\mathcal{C}_1 \subset \mathcal{P}_1$  of the map  $F : \mathcal{C}_1 \rightarrow \mathcal{P}_1$ ,

$$F(\delta_2, \delta_3, \delta_4) = (\text{sign}(\delta_2) [H_{2\varepsilon} \circ S_\tau \circ H_\varepsilon(\tau + |\delta_2|) - H_{2\varepsilon} \circ S_{\tau+|\delta_2|} \circ H_\varepsilon(\tau - |\delta_2|)], \delta'_3, \delta'_4) \quad (6)$$

which is determined by the event sequence

$$E(\mathcal{C}_1) = (s_1)(s_2)(r_1)(r_2, s_3, s_4)(r_3, r_4) \quad (7)$$

or its equivalent with permuted indices  $1 \leftrightarrow 2$ . Here

$$\delta'_i = H_\varepsilon \circ S_\tau \circ J_\varepsilon(H_\varepsilon(\alpha + \tau + \delta_i) + |\delta_2|) + 1 - H_{2\varepsilon} \circ S_\tau \circ H_\varepsilon(\tau + |\delta_2|) - \alpha \quad (8)$$

for  $i \in \{3, 4\}$ , where the phase difference  $\alpha$  between the two synchronized clusters at  $a_1$  is determined by

$$\alpha = H_\varepsilon \circ S_\tau \circ J_{2\varepsilon}(\alpha + \tau) + 1 - H_{2\varepsilon} \circ S_\tau \circ H_\varepsilon(\tau). \quad (9)$$

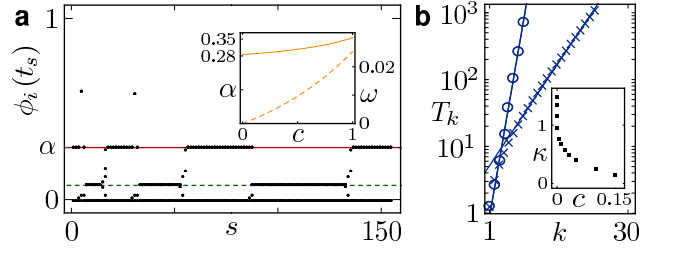


Figure 3: (color online) Heteroclinic switching ( $c > 0$ ). (a) Phases  $\phi_i(t_s)$  (dots) as in Fig. 1a for  $c = 0.05$ . The invariant periodic orbits  $A_i$ , being unstable attractors at  $c = 0$ , still exist for  $c > 0$  (solid and dashed line). Starting in a state near  $A_1$  leads to repeated switching between the two states. Inset: Phase difference  $\alpha$  (9) (solid) and side width  $w$  of the set  $\mathcal{D}'_i$  (11) (dashed) change continuously upon increasing  $c$  from zero. (b) Switching times  $T_k$  to the  $k$ -th switch ( $\times$ :  $c = 0.1$ ,  $\circ$ :  $c = 0.01$ ) increase exponentially with  $k$ , indicating that the dynamics evolve near a heteroclinic cycle between the invariant states. Inset: Fitting  $T_k = \gamma e^{\kappa k}$  to the switching times for several values of  $c$  we find a divergence of  $\kappa$  as  $c \rightarrow 0$ .

For  $|\delta_2| > 0$ ,  $F$  is expanding in the  $\delta_2$ -direction since

$$|(F(\delta))_2| > k |\delta_2| \quad (10)$$

with  $k = \min_{\phi \in [0, 1]} H'_\varepsilon(\phi) > 1$ . For  $\delta_2 = 0$  we obtain a map with the same explicit form as in (6) but with event sequence as in (5) whose domain is a subset of the two-dimensional invariant set  $\mathcal{S}_1 = \{\delta \in \mathcal{P}_1 \mid \delta_2 = 0\}$  where units 1 and 2 are synchronized. States in  $\mathcal{S}_1$  converge to  $A_1$  in the long time limit. Similarly, points in  $\mathcal{S}_2 = \{\delta \in \mathcal{P}_2 \mid \delta_4 = 0\}$  reach  $A_2$  asymptotically.

If the system is locally non-invertible ( $c = 0$ ) the dynamics is as follows (see Fig. 2): Since  $J_\varepsilon(\phi) \equiv 0$ ,  $\delta'_3 = \delta'_4$  according to (8) and hence  $F$  maps  $\mathcal{C}_1$  into two one-dimensional lines  $\mathcal{D}_1 = F(\mathcal{C}_1)$ . Since  $F$  is expanding in  $\delta_2$  (10), all points in  $\mathcal{D}_1 \cap \mathcal{C}_1$  are mapped after a finite number of interactions into  $\mathcal{D}_1 \setminus \mathcal{C}_1$ . The set  $\mathcal{D}_1 \setminus \mathcal{C}_1$  is mapped to  $\mathcal{E}_2 \subset \mathcal{S}_2$  and from there to the attractor  $A_2$ . In Fig. 2 we have plotted a sample trajectory for the switch marked in Fig. 1a. For the positive measure set  $\mathcal{C}_1 \cup \mathcal{S}_1$ , that encloses  $A_1$ , we thus have  $\mathcal{C}_1 \subset \mathcal{B}(A_2)$  and only the zero measure subset  $\mathcal{S}_1$  converges to  $A_1$ . Thus  $A_1$  is an unstable attractor. Permutation symmetry implies analogous dynamics near  $A_2$ . Taken together, for  $c = 0$  the periodic orbits  $A_1$  and  $A_2$  are unstable attractors enclosed by the basins of each other.

If we remove the local non-invertibility ( $c > 0$ ), the dynamics changes qualitatively as shown in Fig. 3: The two periodic orbits  $A_i$  with event sequence (5) still exist, only the phase difference  $\alpha$  changes continuously with  $c$  (Fig. 3a). Starting in a state near one of the  $A_i$  leads to trajectories with switching between both. The switching time increases exponentially with the number of switches (Fig. 3b) indicating that these dynamics originate from an orbit near a heteroclinic two-cycle. Furthermore the switching times diverge as  $c \rightarrow 0$  (cf. Fig. 3b), suggesting

the transition to a network of unstable attractors at  $c = 0$ . Indeed, the structure of the domains of all return maps does not change qualitatively when  $c$  increases from zero. However, since  $J_\varepsilon$  becomes invertible for  $c > 0$ , according to (8) a phase difference  $|\delta_3 - \delta_4|$  shrinks under the return map  $F$ , but does not collapse to zero as for  $c = 0$ ; hence the image  $\mathcal{D}'_1 = F(\mathcal{C}_1)$  stays three-dimensional. It consists of tubes (around the original lines  $\mathcal{D}_1$ ) with a square cross-section of side width

$$w(c) = H_\varepsilon \circ S_\tau \circ U^{-1}(c\varepsilon) - H_\varepsilon \circ S_\tau \circ U^{-1}(0) \quad (11)$$

that continuously increases with  $c$  from  $w(0) = 0$  (Fig. 3a). This reflects the local  $c$ -dependent contraction of the state space according to (6) and (8). All maps with domains that have a non-empty intersection with  $\mathcal{D}'_1$  map  $\mathcal{D}'_1$  to a three-dimensional state space volume around  $A_2$  that is a subset of  $\mathcal{C}_2 \cup \mathcal{S}_2$ . Taken together, states in the three-dimensional set  $\mathcal{C}_1$  evolve to states in a positive measure subset of  $\mathcal{C}_2 \cup \mathcal{S}_2$  that encloses  $A_2$ . Using symmetry again,  $\mathcal{C}_2$  is analogously mapped to a subset of  $\mathcal{C}_1 \cup \mathcal{S}_1$ . This explains the observed switching.

The unstable attractors are converted to non-attracting saddles by locally removing the non-invertibility of the dynamics, which is reflected in the expansion of  $\mathcal{D}_i$ ,  $i \in \{1, 2\}$  to positive measure sets  $\mathcal{D}'_i$  when increasing  $c$  from zero. Moreover, states in the subset of  $\mathcal{C}_1$  with synchronized units 3 and 4, i.e. states in the set  $\{\delta \in \mathcal{C}_1 \mid \delta_3 = \delta_4\}$  are mapped to  $\mathcal{S}_2$  and thus reach the orbit  $A_2$  asymptotically. Hence, this set together with all its image points in  $\mathcal{P}_1$  and  $\mathcal{P}_2$  form a heteroclinic connection from  $A_1$  to  $A_2$ . Thus, by symmetry, the network of two unstable attractors ( $c = 0$ ) continuously bifurcates to a heteroclinic two-cycle ( $c > 0$ ).

The underlying mechanism relies on the interplay of the local instability (10) and the parameter dependent contraction induced by the reset (4), implying the same transition in larger systems (not shown). For locally non-invertible dynamics these display larger networks of unstable attractors [5] with a link between two attractors  $A_i \rightarrow A_j$  if every neighborhood of  $A_i$  contains a positive basin volume of  $A_j$ . Upon lifting the local non-invertibility each link in this network is replaced by a heteroclinic connection.

In summary, we have presented and analyzed the counter-intuitive phenomenon of two unstable attractors that are enclosed by each other's basin volume. We explained this phenomenon by showing that there is a continuous transition from two unstable attractors to a heteroclinic two-cycle. Larger networks of unstable attractors equally show this transition to more complex heteroclinic structures. It constitutes a new type of singular bifurcation in dynamical systems and establishes the first known bifurcation of unstable attractors. Moreover, our results show that this bifurcation occurs upon continuously removing the non-invertibility of the system, whereas both the non-invertible ( $c = 0$ ) and the locally

invertible ( $c > 0$ ) system exhibit equally discontinuous interactions. This explicitly demonstrates that the local non-invertibility and not the discontinuity is responsible for the creation of unstable attractors.

The continuity of the bifurcation has theoretical and practical consequences: For instance, one may investigate features of a system exhibiting heteroclinic switching [6] by studying its limiting counterpart with unstable attractors. Furthermore, this may help designing systems with specific heteroclinic structure, for instance in artificial neural networks, and guide our understanding of time series of switching phenomena in nature, cf. [7]. The associated limiting systems with unstable attractors may not only be analytically accessible, also numerical simulations can be performed in a more controlled way because typical problems with simulations of heteroclinic switching, e.g. exponentially increasing switching times and exponentially decreasing distances to saddles, do not occur if the heteroclinic switching is replaced by networks of unstable attractors.

We thank S. Stolzenberg for help during project initiation. Supported by the Federal Ministry of Education & Research (BMBF) Germany, Grant No. 01GQ0430.

- 
- [1] A. Katok and B. Hasselblatt, *Introduction to the Modern Theory of Dynamical Systems* (Cambridge Univ. Press, 1995); J. Milnor, *Commun. Math. Phys.* **99** 177 (1985).
  - [2] B. Brogliato, *Nonsmooth Mechanics* (Springer 1999); M. di Bernardo et al., *Piecewise-smooth Dynamical Systems* (Springer 2007).
  - [3] Z. Olami, H.J.S. Feder, and K. Christensen, *Phys. Rev. Lett.* **68**, 1244 (1992); J.H.B. Deane and D.C. Hamill, *IEEE Trans. Power Electron.* **5**, 260 (1990); R.E. Mirollo and S.H. Strogatz *SIAM J. Appl. Math.* **50**, 1645, (1990); A.V.M. Herz and J.J. Hopfield, *Phys. Rev. Lett.* **75**, 1222, (1995); W. Senn and R. Urbanczik. *SIAM J. Appl. Math.* **61**, 1143 (2001).
  - [4] M. Timme, F. Wolf and T. Geisel, *Phys. Rev. Lett.* **89**, 258701 (2002).
  - [5] U. Ernst, K. Pawelzik, and T. Geisel, *Phys. Rev. Lett.*, **74**, 1570 (1995); *Phys. Rev. E* **57**, 2150 (1998); M. Timme, F. Wolf, and T. Geisel, *Phys. Rev. Lett.* **89**, 154105 (2002); *Chaos* **13**, 377 (2003).
  - [6] J.H.P. Dawes and T.L. Tsai, *Phys. Rev. E* **74**, 055201(R) (2006); C.M. Postlethwaite and J.H.P. Dawes, *Nonlinearity* **18**, 1477 (2005); R. M. May and W. J. Leonard, *SIAM J. Appl. Math.* **29**, 243 (1975); D. Hansel, G. Mato, and C. Meunier, *Phys. Rev. E* **48**, 3470 (1993); H. Kori and Y. Kuramoto, *Phys. Rev. E* **63**, 046214 (2001); P. Ashwin and J. Borresen, *Phys. Rev. E* **70**, 026203 (2004); P. Ashwin et al., *Phys. Rev. Lett.* **96**, 054102 (2006).
  - [7] P. Ashwin and M. Timme, *Nature* **436**, 36 (2005).
  - [8] P. Ashwin and M. Timme, *Nonlinearity* **18**, 2035 (2005).
  - [9] C. Kirst, T. Geisel, and M. Timme, e-print arXiv:0810.2749v1 (2008).
  - [10] M. Krupa, *J. Nonlinear Sci.* **7**, 129 (1997).